Microwave inverse free-electron-laser accelerator using a small "phase window"

T. B. Zhang and T. C. Marshall
Department of Applied Physics, Columbia University, New York, New York 10027
(Received 22 March 1994)

We analyze, by numerical simulation, an inverse free-electron-laser accelerator for the purpose of accelerating electrons from 1.5 MeV to about 20 MeV in a 1.5 m long undulator ($\sim$13 MeV/m). The initial phase distribution of injected electrons is chosen to lie in a small "phase window" from $-\pi/8$ to $-3\pi/8$ so that all the electrons can be trapped in the accelerating bucket. In this case, there is little particle spread in phase space and the electron energy spectrum is a narrow spike.

PACS number(s): 41.60.Cr, 41.75.Ht, 29.17.+w

I. INTRODUCTION

The free-electron laser (FEL) has proved to be a very efficient tunable radiation source. If we regard the FEL as an electron "decelerator" where the energy of electrons is transferred in the undulator to amplify electromagnetic radiation, then it is very natural to take advantage of the analogy between FEL devices and radio frequency accelerators in which a high power electromagnetic field is used to accelerate an electron beam from low energy to high energy. The FEL operated in this process is called the inverse free-electron-laser accelerator (IFELA). The principle of the IFELA was described many years ago [1], and has been reexamined in more detail both theoretically [2,3] and experimentally [4] in the last few years. It appears to offer some promise for the improvement of a practical "advanced" accelerator.

The principle of acceleration is as follows. In the rest frame of the electron beam, the magnetostatic periodic field of the undulator (or wiggler) is transformed into an electromagnetic wave that beats with the microwave source; acceleration occurs by trapping a bunch of electrons into the resulting ponderomotive wave, and then increasing the velocity of this wave by tapering the undulator field and/or amplitude. We can identify some of the problems facing the IFELA by considering the acceleration mechanism:

$$\frac{d\gamma}{dz} = -a_s \frac{\omega_s}{c} \frac{a_w}{\gamma} \sin\psi \ , \tag{1}$$

where γ is the relativistic factor of electron, $a_s = eA_s/mc^2$ is the normalized vector potential of the radiation field, ω_s is the radiation frequency, a_w/γ involves the normalized vector potential of the undulator field and amounts to the ratio of electron velocity perpendicular to the axis to the velocity parallel to the axis of the device, and is caused by the undulator interaction with the electrons. ψ is the relative phase of the electron with respect to the rf driving field.

It can be seen from (1) that the relative phase ψ plays an important part in the FEL. When $\psi > 0$, $d\gamma/dz < 0$ and this case represents stimulated emission, as in the FEL. When $\psi < 0$, then $d\gamma/dz > 0$ and this case represents stimulated absorption which is called the inverse FEL process. We can inject the electrons into a small "phase window" so that all the electrons are located in the accelerating buckets. This can be done in our example because the acceleration power is obtained from a microwave source that has a "long wavelength" (unlike some IFELA's that use a laser source of power). In our simulation the small "phase window" of phase angles is between $-\pi/8$ and $-3\pi/8$. This can be done in practice by gating the injected electron beam emerging from a rf gun and buncher cavity as it enters the IFELA; the $\pi/4$ spread corresponds to a pulse length of $\sim$6 psec. In further consideration of (1), we find that a strong rf electric field ($\sim$1 MeV/cm—below the vacuum breakdown limit) is required, as well as a strong transverse undulator magnetic field ($\sim$1 T), in order to achieve a sizable accelerating gradient.

This work was done in connection with a project to study whether the IFELA could make a potentially attractive electron accelerator with output energy $\sim$20 MeV. The authors acknowledge their interactions with other participants who contributed to the entire design study [5] (see Acknowledgment).

II. THEORETICAL MODEL

We present in this section the basic theoretical model used to describe the acceleration process in an IFELA. The system uses a helical undulator and circularly polarized driving field that propagates in a cylindrical waveguide. The fundamental equations used herein to describe the IFELA interaction are the well-known FEL equations [6,7] that define the energy and relative phase of a resonant electron in terms of the undulator magnetic field, the undulator period, and the driving field.

$$\frac{d\gamma_j}{dz} = -\frac{a_w a_s \frac{\omega_s}{c}}{\gamma_j} \sin(\psi_j) \left[1 - \frac{\mu^2 - 2a_w a_s \cos\psi_j}{\gamma_j^2} \right]^{-1/2} , \tag{2}$$

$$\frac{d\psi_j}{dz} = k_w + k_s - \frac{\omega_s}{c} \left[1 - \frac{\mu^2 - 2a_w a_s \cos\psi_j}{\gamma_j^2} \right]^{-1/2} + \frac{\partial\phi}{\partial z} \ . \tag{3}$$

Here $\mu^2=1+a_w^2+a_s^2$, z is the axial distance along the system and is the independent variable. γ_j is the relativistic factor of the jth electron, ψ_j is the phase of the jth electron with respect to the driving field, ϕ is the phase shift of the driving radiation field.

The driving field equation is a solution of the Maxwell's equations. It has the following form

$$\left[\nabla_\perp^2+2ik_s\frac{\partial}{\partial z}-\delta k_s^2\right]u(r,z)=-\frac{\omega_p^2}{c^2}\left\langle\frac{e^{-i(\psi-\phi)}}{\gamma}\right\rangle , \quad (4)$$

$$\delta k_s^2=k_s^2-\frac{\omega_s^2}{c^2} . \quad (5)$$

The angular brackets in the right-hand side of Eq. (4) indicates an ensemble average over all electrons. Equation (4) can be solved with the cylindrical waveguide boundary conditions.

Equations (2)–(4) comprise a complete set of nonlinear coupled equations. The motion Eqs. (2) and (3) are valid for every electron, and given the initial conditions $\psi(0)$ and $\gamma(0)$ for every electron along with the parameters of the undulator, these equations can be integrated numerically to yield the value of ψ and γ as a function of the longitudinal position z. The motion of the electron in the undulator and a guiding magnetic field (used for beam transport) is represented by the term a_w/γ, and is obtained by separate solution of the orbit equation [8,9].

$$\beta_\perp=\frac{2\Omega_\perp\dfrac{I_1(\lambda)}{\lambda}\beta_\parallel}{\Omega_0-\gamma k_w c\beta_\parallel\pm 2\Omega_\perp I_1(\lambda)} , \quad (6)$$

where $\lambda=\pm\beta_\perp/\beta_\parallel$, $\beta_\perp$ and $\beta_\parallel$ are the transverse and axial velocities of electrons respectively; $\Omega_\perp$ and Ω_0 are the gyrofrequencies of electrons in the undulator and guiding fields; $I_1(\lambda)$ is the first-order Bessel function of imaginary argument.

The driving field, which is coupled with the equations of motion through $u(r,z)\equiv a_s e^{i\phi}$ in the right hand of (2) and (3), is also a self-consistent solution to this set of equations. The procedure we used here is to solve the coupled Eqs. (2)–(4) and obtain the final coordinates in phase space for every particle. The electrons are initially spread in 20 strips in the range of beam radius, with one thousand particles in each strip, all the particles being monoenergetic and having initial phase uniformly distributed within the small "phase window." The code we use is based on the equations above with a one-dimensional description for the motion of electrons, but it is two dimensional for the driving field dynamics. This is a single-pass code corresponding to the Compton regime, for which the space charge effect is not considered: this approximation is satisfactory if the electron beam current is not higher than 100 A.

III. SIMULATION RESULTS AND DISCUSSION

The parameters used in the simulations are listed in Table I and are close to those of a proposed accelerator at Yale University. The rf for the cavity injector is obtained as a subharmonic of the microwave source, or a 2.85 GHz high power klystron; this power can be converted [10] to the seventh harmonic at 20 GHz so as to drive the IFELA [Fig. 1(a)]. We imagine that the waveguide will fill with microwaves for several nsec, interacting with a reflector in the waveguide so as to build up a high intensity field for electron acceleration ($Q\sim 5000$) . Then the subharmonic cavity will inject a short pulse of electrons into the IFELA, which will absorb the rf energy [Fig. 1(b)]. The TE_{11} mode was chosen since it has a lowest cutoff frequency. In the numerical study, we increase the undulator period and the axial guiding field linearly in the accelerating section. The gradient of the axial field is determined so that the accelerator works with the stable group I electron orbits [8,9].

In order to obtain the correct axial profile of the undulator magnetic field (or a_w/γ), it was found necessary to vary the winding depth of the undulator current winding, since the current through the winding should be held constant. An accurate calculation of the on-axis undula-

TABLE I. IFELA simulation parameters.

Beam parameters	
Electron beam energy	$\gamma=4.0$–44.0
Electron beam current	$I_b=10.0$ A
Electron beam radius	$r_b=0.2$ cm
Undulator parameters	
Undulator magnetic field	$B_s=(3.0-10.7)\times 10^3$ Gauss [Fig. 1(a)]
Guiding field	$B_0=(0.1-1.5)\times 10^3$ Gauss; linear ramp
Undulator period	$l_w=4.9$–10.5 cm; linear ramp
Undulator taper	$\eta=0.0075$ cm^{-1}
Undulator length	$L=150$ cm
Effective undulator parameter	$a_w=2.0$–12.2
Driving field and waveguide parameters	
Driving field wavelength	$\lambda_s=1.5$ cm
Driving field intensity	$a_{s0}=0.35$ (circular polarized)
Waveguide mode	TE_{11}
Waveguide radius	$R=1.0$ cm

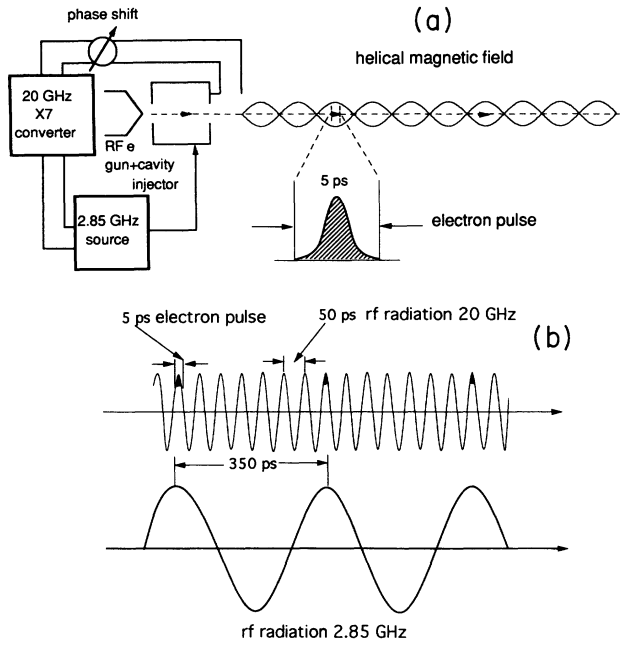

FIG 1. (a) Schematic of the microwave IFELA, showing the microwave feed to the gun and the accelerator. (b) rf wave forms, showing how the bunch is formed and synchronized in the IFELA.

tor field has been made by Park *et al.* [11]. We determine the undulator field by interaction with the acceleration equations, and then find the wire winding radius that will give the desired field: Fig. 2(a) shows the field and Fig. 2(b) shows the winding radius that provides this field, using a current of 38.5 kA. This field, together with the guiding field and undulator period, will maintain the resonant phase condition that will accelerate the electrons.

Figure 3 shows the electron energy as a function of IFELA axial distance. The electrons are injected monoenergetically at $\gamma=4$ with phase distribution between $-\pi/8$ and $-3\pi/8$. The resonant energy of the given hardware design is shown in dotted line and can be determined by Eq. (3) as

$$\gamma_r = \left[\frac{(k_w+k_s)^2(1+a_w^2)}{(k_w+k_s)^2-\dfrac{\omega_s^2}{c^2}} \right]^{1/2} . \tag{7}$$

To get the optimum accelerating gradient, Eq. (7) must be obeyed so that a strong beam-wave interaction occurs in the whole acceleration process. The functional forms of $k_w(z)$ and $a_w(z)$, i.e., the undulator period and undulator field, are very important for the match up of the electron energy and the resonant energy. We vary the parameters of undulator so as to gradually increase the resonant energy of the trapped electrons and put most beam electrons into an accelerating bucket. It can be seen from Fig. 3 that the beam energy and the resonant energy match quite well in the whole acceleration section.

At the end of the IFELA, we allow the guiding field to decrease gradually, while maintaining the strong undulator field. With a sufficiently gentle gradient, one can show that the defocusing effect of the decreasing guide field can be overcome by the natural focusing of the helical undulator. If we leave the rf field on in this end section of the IFELA, we find there is still a small increase of electron energy since the electrons are still in the accelerating buckets. After that, with the decrease of guide field, a_w/γ drops, and the electrons fall out of resonance. Since the electrons have random phase with respect to the driving field, no net energy increase occurs in the end section. In this way, the output beam of the IFELA can be obtained in zero guiding field.

Shown in Fig. 4 is a_w/γ, the transverse velocity parameter of the electrons. Higher accelerating gradient requires larger a_w/γ, which is about 0.5 at the beginning of

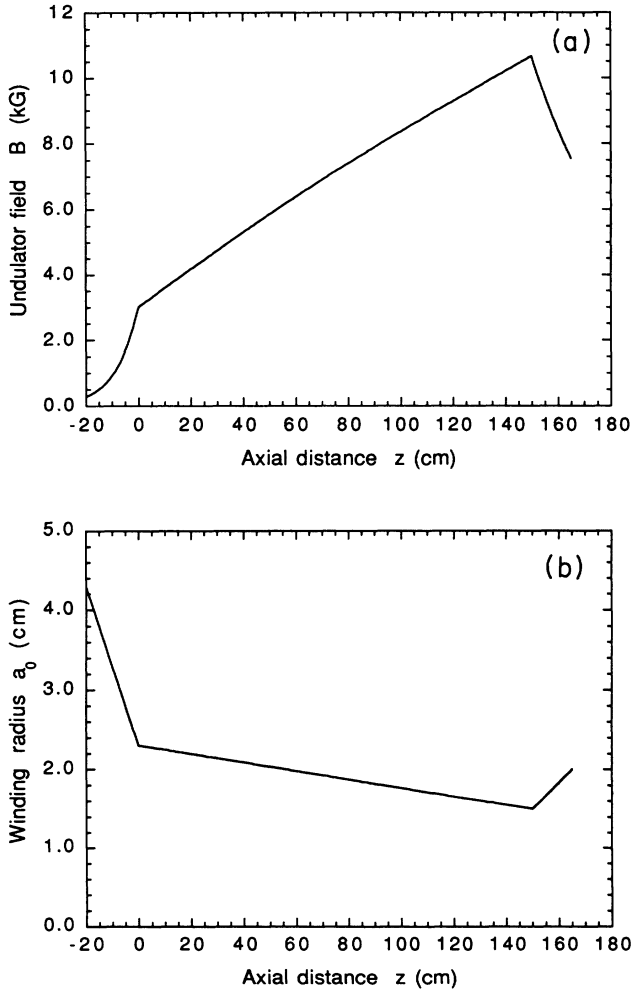

FIG. 2. (a) Axial profile of the undulator field. The region $z<0$ is the adiabatic entry into the undulator, and the region $z>150$ cm is the exit region of the IFELA. The current in the winding is 38.5 kA, the undulator period varies as given by Table I, and the winding coil radius varies as given in (b). (b) The winding radius of the undulator coil which gives the field profile of (a), given a constant current of 38.5 kA.

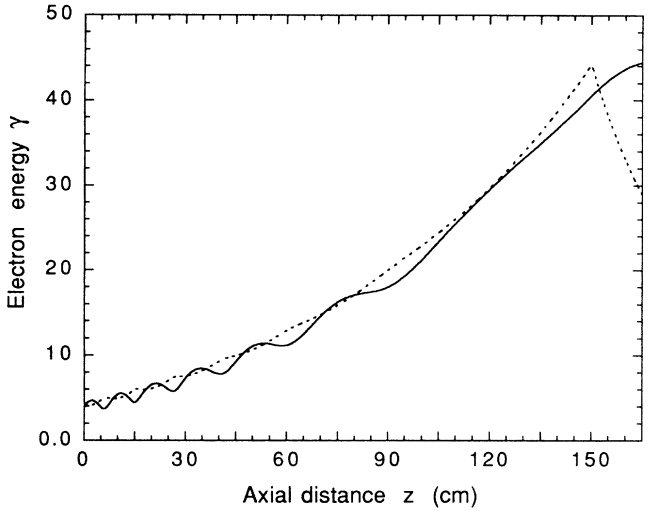

FIG. 3. Electron energy as a function of the axial distance along the undulator. The dotted line is the resonant energy of trapped particles for the given IFELA parameters. Initial injection is a cold beam at $\gamma=4$ with phase between $-\pi/8$ and $-3\pi/8$.

the undulator. The oscillation of this parameter at the beginning comes from the bunching effect in the first several periods of the undulator.

The ultimate electron energy γ_L can be estimated as follows. Under resonant conditions, Eq. (1) implies the inequality

$$\gamma_L \leq \left[\frac{4\pi a_s \overline{a_w}}{\lambda_s} L\right]^{1/2}, \tag{8}$$

$\overline{a_w}$ is the average undulator parameter, L is the length of the undulator. Substituting the parameters in Table I, we find that γ_L is about 50, which is very close to the simulation result.

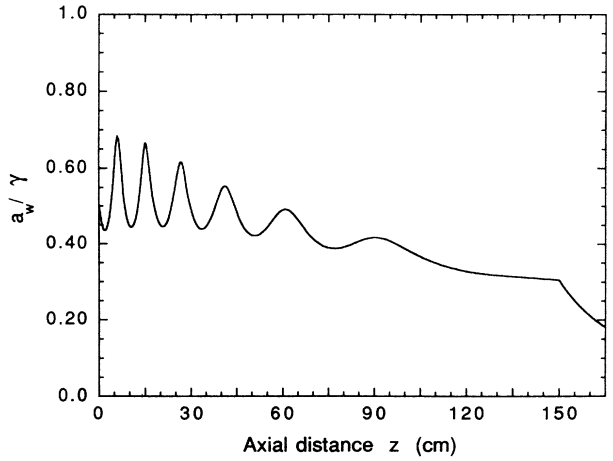

FIG. 4. Transverse electron velocity parameter as a function of undulator axial distance.

Figure 5 shows the phase plot and the energy spectrum of the accelerated electrons at the end of the accelerating section. The initial phase distribution is between $-\pi/8$ and $-3\pi/8$, and because of this small "phase window," all the electrons we simulated are trapped in the accelerating bucket with the phase between $-\pi/2<\psi<0$. In the phase plot there is no spread of the particles, and the electron energy distribution in this case is also a narrow spike.

To compare with the above results, Fig. 6 shows the phase plot and the energy spectrum of the accelerated electrons when the injected electrons are uniformly distributed between $-\pi$ and π. The conditions for this example again correspond to Table I. At the beginning of the undulator, the electrons with relative phase $\psi>0$ will be decelerated, whereas only those with $\psi<0$ can be accelerated. Since the undulator parameters are designed

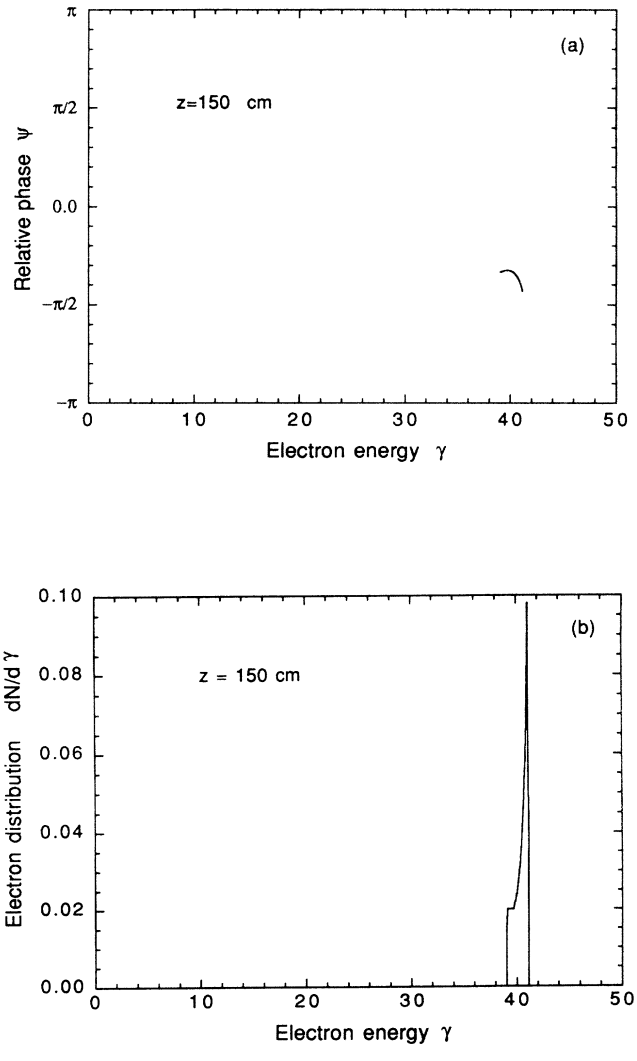

FIG. 5. The electron distribution in phase space (a) and energy spectrum (b). The initial phase distribution is between $-\pi/8$ and $-3\pi/8$. Conditions are obtained from Table I and Fig. 2.

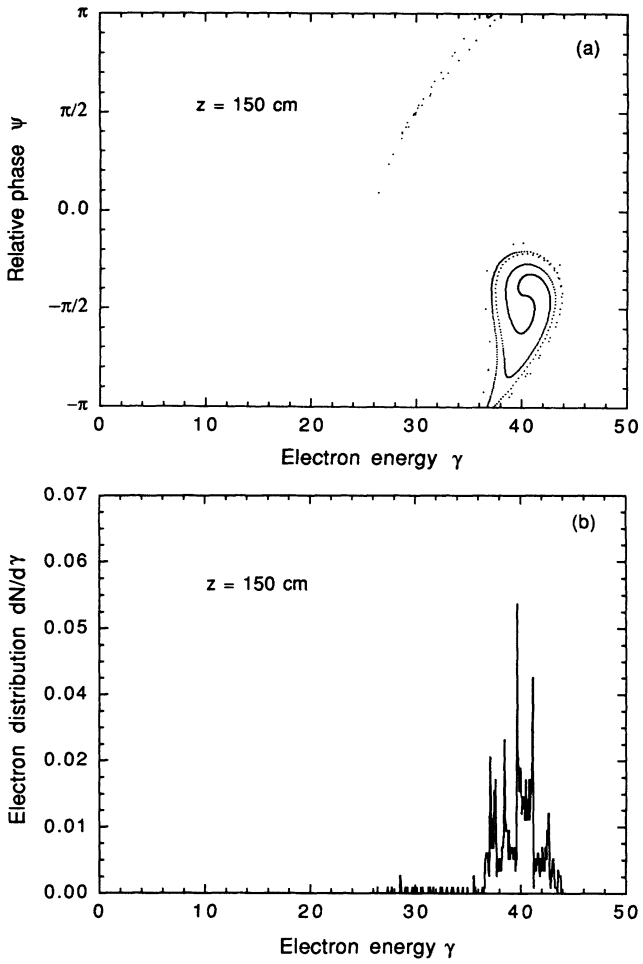

FIG. 6. The electron distribution in phase space (a) and energy spectrum (b). The initial electrons are uniformly distributed from $-\pi$ and π; otherwise, the conditions are obtained from Table I and Fig. 2.

so that most of the electrons will be accelerated, after several undulator periods we find a large fraction of electrons are trapped in the accelerating bucket, while about thirty percent of electrons have escaped the potential well. In phase space the electrons are localized in an area which is much larger than the small "phase window" case, and so the energy spectrum is a wide distribution.

In summary, we have developed a computer code to simulate the acceleration process in the inverse free-electron-laser accelerator. We find that by using a small "phase window" for the initial phase distribution of electrons, all the electrons can be trapped in the potential well of the accelerating ponderomotive field and can be accelerated to the end of the undulator. Furthermore, because there is no particle loss and spread, the final energy spectrum is a narrow spike. Further improvement in beam energy spread can be obtained at the expense of the bunch length in the end section of the device by manipulating the bucket so as to "condition" the beam. The narrow phase spread of $\pi/4$ in our example implies a bunch length of 2 mm or 6 psec, which is readily obtained from an rf cavity injector. (However, for an IFELA driven by a short-wavelength laser, the injected electrons are spread over the entire range of 2π.)

The accelerating gradient we have obtained in this example is ~ 13 MeV/m, comparable with the best rf linac performance. A higher gradient, perhaps ~ 100 MeV/m, could be obtained in an IFELA that uses a short wavelength laser which is focused onto the axis of a filamentary electron beam (e.g., 10 μ laser and 40 MeV beam energy) [12]; the Rayleigh range of the diffraction is then taken to be the same size as the undulator. In our example, microwaves are used in conjunction with a waveguide, and so the "focusing" is not possible because of the longer wavelength and hence the accelerating gradient is less.

ACKNOWLEDGMENTS

This work is sponsored by the U.S. Department of Energy and Omega-P Inc. The authors acknowledge many useful discussions with J. Hirshfield, P. Sprangle, and A. Ganguly in the course of this work.

[1] R. B. Palmer, J. Appl. Phys. **43**, 3014 (1972).
[2] A. C. Ting and P. Sprangle, Part. Accel. **22**, 149 (1987).
[3] S. Y. Cai and A. Bhattacharjee, Phys. Rev. A **42**, 4853 (1990).
[4] I. Wernick and T. C. Marshall, Phys. Rev. A **46**, 3566 (1992); see also A. Fisher, J. Gallardo, J. Sandweiss, and A. van Steenbergen, in *Advanced Accelerator Concepts,* edited by J. Wurtele, AIP Conf. Proc. No. 279 (AIP, New York, 1993), p. 292.
[5] A. K. Ganguly *et al.*, Bull. Am. Phys. Soc. **39**, 1012 (1994).
[6] N. M. Kroll, P. L. Morton, and M. N. Rosenbluth, IEEE J. Quantum Electron. **QE-17**, 1436 (1981).
[7] A. Bhattacharjee, S. Y. Cai, S. P. Chang, J. W. Dodd, A. Fruchtman, and T. C. Marshall, Phys. Rev. A **40**, 5081 (1989).
[8] L. Friedland, Phys. Fluids **23**, 2376 (1980).
[9] A. K. Ganguly and H. P. Freund, Phys. Rev. A **32**, 2275 (1985).
[10] A. K. Ganguly and J. L. Hirshfield, Phys. Rev. Lett. **70**, 291 (1993).
[11] S. Y. Park, J. M. Baird, R. A. Smith, and J. L. Hirshfield, J. Appl. Phys. **53**, 1320 (1982).
[12] A. Fisher, J. Gallardo, J. Sandweiss, and A. van Steenbergen, in *Advanced Accelerator Concepts* (Ref. [4]), p. 299.